



## Efficient Image Registration Using Discrete Orthogonal Stockwell Transform and SIFT

Hossam-E M. Shamardan<sup>1\*</sup>

<sup>1</sup>Department of Information Technology, Faculty of Computers and Information Systems, Helwan University, Cairo, Egypt.

### Author's contribution

The sole author designed, analyzed and interpreted and prepared the manuscript.

### Article Information

DOI: 10.9734/JAMCS/2018/40026

#### Editor(s):

- (1) Kai-Long Hsiao, Associate Professor, Taiwan Shoufu University, Taiwan.  
(2) Qiang Duan, Associate Professor, Information Sciences & Technology Department, The Pennsylvania State University, USA.

#### Reviewers:

- (1) Ayush Dogra, Panjab Univehrsity, India.  
(2) Xiangzeng Liu, Xi'an Microelectronics Technology Institute, China.  
(3) Rajnish K. Ranjan, Govt. Women Polytechnic, India.  
Complete Peer review History: <http://www.sciencedomain.org/review-history/23885>

Received: 12<sup>th</sup> January 2018

Accepted: 21<sup>st</sup> March 2018

Published: 29<sup>th</sup> March 2018

Original Research Article

## Abstract

Image registration is a vital step for most of recent image processing applications. In this paper, a novel approach for magnetic resonance images (MRI) registration based on artificial neural network (ANN) is proposed. The ANN achieves the state-of-the-art performance for estimation problems, hence it has been adopted for estimating the registration parameters. The ANN is fed by joined features extracted from both of spatial and frequency domains. The Scale Invariant Feature Transform (SIFT) is used for extracting the spatial domain features while The Discrete Orthogonal Stockwell Transform (DOST) coefficients are used as frequency domain features. The combined features provide a robust foundation for the registration process. Many experiments were performed to test the success of the new approach. The simulation results demonstrate that the proposed approach yields a better registration performance with regard to both the accuracy, and the robustness versus noise conditions.

*Keywords:* DOST; SIFT; neural network; image registration; geometric parameters.

\*Corresponding author: E-mail: [hossam@fci.helwan.edu.eg](mailto:hossam@fci.helwan.edu.eg);

## 1 Introduction

Image registration is the positioning of two or more images captured at different times by one sensor or more, to have the same location. This step is considered fundamental for a multiple of application such as remote sensing and medical applications. For example, medical image applications are required by medical doctors in order to provide accurate and complete information about the patients. For example, MRI images offer information on the formation of internal tissues such as muscles, and capillary. Image registration help doctors to recognize, and follow the changes undergoing to their patients. The image registration is the process of relating images captured from different temporal and/or spatial sensors in order to ensure accurate alignment between given points in all images [1-2].

Image registrations methods are divided broadly into Intensity-based, and feature-based methods. The process registration of two images, consider one image to be the source image and it is fixed and a new image, the target image, that is subject to geometrical transformation in addition to distortion and, noise. Intensity methods rely on finding the relationships of the intensities between the two images through applying correlating measurement tools. Feature-based methods rely on extracting reliable, and accurate features from the source and target images, finally matching the similar features between the source and target. A map between the source and target images eventually can be estimated thereby building pixel to pixel association. It is required for those features to be robust, distinctive, accurate, and computationally inexpensive [3].

Mapping every pixel in the target image to every pixel in the source image is the foundation of the image registration process. The successful mapping requires finding the accurate geometric transformations to transform the target image into the source image. Estimating the affine transformation parameters would result in the registration of the two images by applying an inverse affine transform on the target image. Thereby, image registration can be considered as a problem of transformation parameter estimation of the target image [4-5].

In general, affine transformations involve basic operations: rotation, scaling and, translation and any other operations such as reflection, shearing is considered a combination of any of basic operations. According to the literature [6], Transformation combinations are described in terms of matrix operations. To use matrix operations, homogeneous coordinates are utilized since they enable all affine operations to be expressed as a matrix multiplication.

The 2D affine transformations matrix  $T$  maps coordinates of source image pixel into new coordinates  $(x, y) \rightarrow (x', y')$  as indicated in Eq. (1).

$$\begin{pmatrix} x' \\ y' \\ 1 \end{pmatrix} = \begin{pmatrix} a & b & c \\ d & e & f \\ 0 & 0 & 1 \end{pmatrix} \begin{pmatrix} x \\ y \\ 1 \end{pmatrix} \quad (1)$$

Where  $T$  is a transformation matrix 3\*3, and the pixel located at  $(x, y)$  is represented by a homogenous coordinated as a triplet  $(x, y, 1)$ . The transformation matrix  $T$  can be formed according to the required transformation as shown in Fig. 1.

$$\begin{matrix} \begin{pmatrix} \cos(\theta) & \sin(\theta) & 0 \\ -\sin(\theta) & \cos(\theta) & 0 \\ 0 & 0 & 1 \end{pmatrix} & \begin{pmatrix} s_x & 0 & 0 \\ 0 & s_y & 0 \\ 0 & 0 & 1 \end{pmatrix} & \begin{pmatrix} 0 & 0 & \Delta_x \\ 0 & 0 & \Delta_y \\ 0 & 0 & 1 \end{pmatrix} \\ (a) & (b) & (c) \end{matrix}$$

**Fig. 1. (a) Rotation (b) Scaling (c) Translation matrices**

Most of image registration methods as indicated by [7] have four major steps as shown in Fig. 2:

- Feature Extraction: Distinctive items in an image are extracted manually or automatically. Features can include edges or lines. These features are represented by their identification descriptors [8-9].
- Feature Corresponding: In this step, the detected features in both of the reference image and those in the target image are compared and an establishing correspondence between those features is determined. For this goal, Feature descriptors similarity measuring tools are used.
- Transformation Parameters Estimation: the feature Corresponding step results in estimating the transformation parameters. The transformation parameters are used to establish a mapping function to be used for aligning the target image with the source image.
- Target Image Inverse Transformation: according to the established map in the previous step, the target image is inversely mapped and Resampled and Transformation
- 

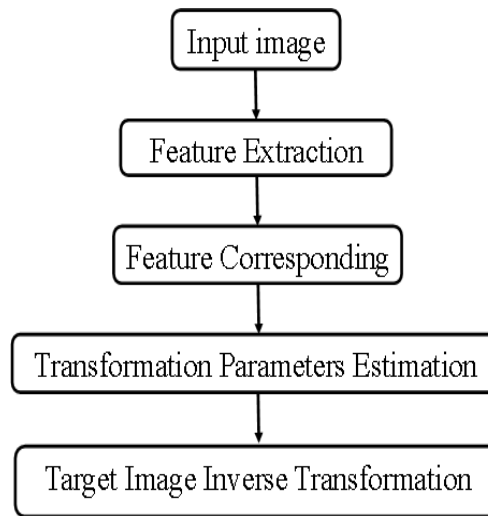


**Fig. 2. Features based image registration system**

Image feature selection is crucial step through the registration process and preparatory for the feature correspondence step. Features should be distinctive, robust, and distinguishable. Selecting weak or irrelevant features will not permit building precise transformation model, eventually will not yield inverse transformation to retrieve the exact locations of the pixels in the target image [8]. A detailed description of the feature selection problem and its consequences was described in [5].

Image features are classified into two classes, spatial and frequency. The spatial domain features are extracted by finding the distinctive and noticeable objects such as points, edges, corners, or lines. In medical, and remote sensing application where images contain significant and easily distinguishable objects, the spatial features are suggested [10]. On the other hand, this class of features suffers from drawbacks which are its sensitivity to scaling and therefore, and difficult to establish a correspondence between two different images [11]. Moreover, most medical images may include just a single particular object and these images are usually believed to suffer from fewer details in spatial domain [5].

The second class of frequency-based features has been investigated extensively as a base for image registration approaches. The Fast Fourier Transform (FFT) provides basic features that can be used for estimating basic geometric transformation parameters [12]. Similar to FFT the Discrete Cosine Transform (DCT) has been studied in [13] and are considered computationally at low-cost. The Discrete Wavelet Transform was used as well for registration in [14] and a complete study for the performance of DWT

combined with features in spatial domain was given in [15]. Features in the frequency domain can achieve image registration with better advantages such as big scaling and rotation parameters [16].

SIFT algorithm is considered the state-of-art for one of the important methods to find spatial domain features in the image that is invariant to scaling, orientation, affine transforms and illumination changes. These advantages make SIFT very relevant, and desirable for image registration approaches. Besides these advantages, SIFT technique has some limitations that cause a large number of mismatches that greatly affect the process of registration [9,17]. Combining features from spatial domain (SIFT) and frequency domain (DCT or DWT) provide robust feature base for image registration [5,15].

Using SIFT and frequency domain based features for training a neural network for image registration has obtained more consideration in modern researches [5,15,18,19]. Classical methods of image registration can estimate the transformation parameters individually at a time where the neural network can determine all the transformation parameters simultaneously. When the neural network is trained, only the computation in the forward direction is required to obtain all the transformation parameters together. Another benefit of using neural networks is that they are capable to find a nonlinear relationship between input/output due to their non-linear activation functions, which allow neural networks to handle the cases of more complicated transforms.

This paper provides a novel approach for image registration. The approach adopts the ANN as geometric parameter estimation tool. The ANN is trained on patterns of features for transformed images. The ANN is utilized for its capability to find the complex relationship between the output (transformation parameters) and the input (features pattern). Both of spatial and frequency based features were used, namely the SIFT and the DOST.

The rest of the paper is organized as follows. The proposed algorithm structure and its background review are discussed in section 2. Section 3 the simulation setup and the results are elaborated. The overall conclusion and the future work is presented in section 4.

## 2 The Proposed Algorithm

In this section, the structure of the new proposed algorithm will be discussed in details in section 2.1. The DOST (Discrete Orthogonal Stockwell Transform), and the SIFT (Scale Invariant Feature Transform) will be reviewed at sections 2.2 and 2.3 respectively

### 2.1 The proposed algorithm structure

The proposed algorithm is training a feed-forward neural network. The training is performed through a feedforward neural network that contains hidden layers with neurons. The training pattern is composed of two combined parts. The first part contains the 2D DOST frequency components. The second part of the pattern is the SIFT descriptors. Both of the frequency components part and the SIFT part are computed at every affine transformation and fed into the neural network as shown in Fig. 3. After the training of the ANN, any target image which contains unknown transformation parameters is fed into the ANN and the resulting output represents the real parameters.

The target contains the five basic affine transformation parameters which are  $\theta$ , representing the rotation angle,  $s_x$ ,  $s_y$  representing the scaling factors in x and y directions respectively and, finally  $\Delta_x$ ,  $\Delta_y$  which representing the translation in x and y directions respectively.

To register an image, its affine parameters are estimated by calculating its feature and passing it to the trained neural network resulted from the first phase. To examine the proposed algorithm, the experiments include extracting features from other frequency domains, namely, DCT and DWT.

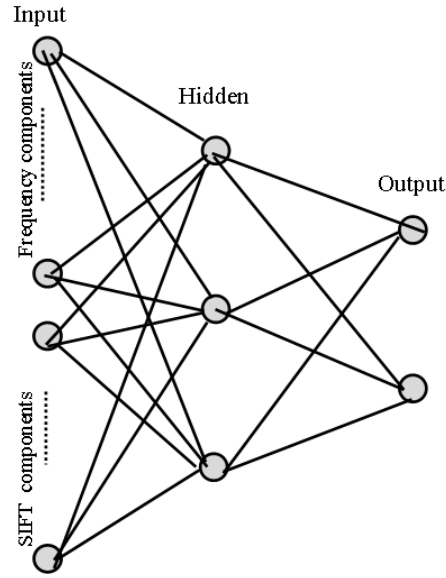


Fig. 3. The structure of the used neural network

## 2.2 DOST (Discrete orthonormal stockwell transform)

The DOST is a trimmed version of the fully redundant Discrete Stockwell Transform (DST) [20]. The DOST provides lesser sampling rates for lower frequencies and higher sampling rates for higher frequencies to solve the DST redundancy. The DOST defines a group of  $N$  orthogonal unit-length basis vectors, each of them aims a specific area in the time-frequency domain. The areas defined by DOST are described by a set of parameters:  $\nu$  specifies the center of each frequency strip (voice)  $p$ ,  $\beta$  is the width of that strip and  $\tau$  specifies the location in the time axis. DOST basis vectors for a particular strip  $p$  and the parameters describing these basis vectors are defined as:

$$S(kT)_{[\nu, \beta, \tau]} = \frac{1}{\sqrt{\beta}} \sum_{f=\nu-\beta/2}^{\nu+\beta/2-1} e^{(i2\pi \frac{k}{N} f)} e^{(-i2\pi \frac{\tau}{\beta})} e^{(-i\pi\tau)} \quad (2)$$

For  $k = 0, 1, \dots, N - 1$ , which can be summed analytically to:

$$S(kT)_{[\nu, \beta, \tau]} = ie^{(-i\pi\tau)} \frac{e^{-2i\alpha(\nu-\beta/2-1/2)} - e^{-2i\alpha(\nu+\beta/2-1/2)}}{2\sqrt{\beta} \sin(\alpha)} \quad (3)$$

Where  $\alpha = \pi(k/N - \tau/\beta)$  is the center of the temporal window and  $\nu$  depicts the center of each frequency strip voice with a bandwidth of  $\beta$ . In order to cause the basis vectors in (3) orthonormal, the parameters,  $\beta$ ,  $\nu$  and  $\tau$ , have to be chosen properly. Let the variable  $p$  denote the level of spatial decomposition. Stockwell in [20] defines DOST basis functions for each level  $p$  as indicated in Equation (4):

An example of ordered DOST coefficients in the frequency-time domain is shown in Fig. 4. The DOST coefficients are calculated for a signal of length 16 and it is obvious that the DC coefficient is located at

$$\begin{aligned}
 p &= 0, \quad \mathcal{S}(kT)_{[v,\beta,\tau]} = 1, \\
 p &= 1, \quad \mathcal{S}(kT)_{[v,\beta,\tau]} = e^{(-2ik\pi/N)}, \\
 p &= 2, \dots, \log_2(N) - 1, \text{ pick:} \\
 v &= 2^{(p-1)} + 2^{(p-2)}, \\
 \beta &= 2^{(p-1)}, \\
 \tau &= 0, \dots, \beta - 1.
 \end{aligned} \tag{4}$$

the middle of the frequency axis(  $N/2$  ). The distribution of the DOST coefficients locations through

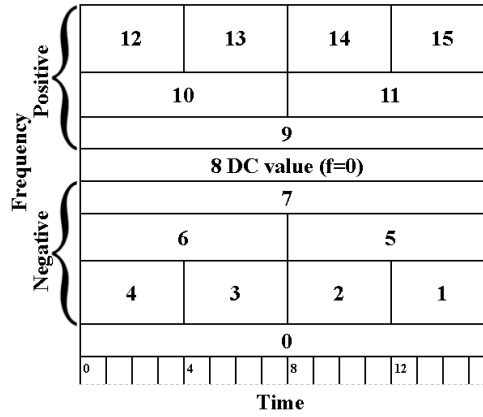


**Fig. 4. The order of DOST coefficients for  $N$  elements vector into Frequency-Time space**

The Time-Frequency domain indicates a symmetric correspondence between the positive and negative-frequency coefficients in the 1-D representation. That is, for a given coefficient with index  $i$  in the 1-D DOST vector, its negative-frequency analogue is at index  $N - i$ . This indexing convention will help later to gain symmetry of the DOST [21]. Selecting  $M$  coefficients from the DOST spectrum is executed by including the coefficients in the range:  $N/2 \rightarrow N/2 + M - 1$

Similar to 1D-DOST, The 2D-DOST of the image  $h[x, y]$  is defined by dividing the Fourier transform of the image 2D-FT of the image,  $H[m, n]$ , multiplying by the square root of the number of points in the partition ( $\beta$ ), and performing an inverse 2D-FT as indicated in equation (5).

$$\mathcal{S}[x', y', v_x, v_y] = \frac{1}{\sqrt{2^{p_x + p_y - 2}}} \sum_{m=-2^{p_x-2}}^{-2^{p_x-2}-1} \sum_{n=-2^{p_y-2}}^{-2^{p_y-2}-1} H(m + v_x, n + v_y) e^{2i\pi\left(\frac{mx'}{2^{p_x-1}} + \frac{ny'}{2^{p_y-1}}\right)} \tag{5}$$

Where  $v_x = 2^{p_x-1} + 2^{p_x-2}$  and  $v_y = 2^{p_y-1} + 2^{p_y-2}$  are representing the horizontal and vertical voice frequencies [22]. As aforementioned, the DC coefficient has located the middle of the positive frequency axis. To select  $M_x * M_y$  from the DOST coefficients, a rectangle starting from the DC coefficient is built and its coefficients are acquired as the needed features.

## 2.3 SIFT (Scale invariant feature transform)

SIFT has been provided as a feature matching tool and applied effectively into modern image processing applications such as image registration, and object recognition [9]. The major advantage of using SIFT to extract features is that the generated features are invariant to rotation, scaling, and translation, and as well as SIFT provides robustness to perspective changes. The SIFT algorithm has been used extensively in image registration problems in the literature [17,18,22]. The four main steps to calculate SIFT are:

### 1. Scale-space and extrema detection

The first step is to build the scale space of an image by applying the “Difference of Gaussian” function to find the maxima and the minima. This step target is to search among all scales to find all the possible positions of interest points which are invariant to scale and orientation. The verification of the interest point is established by comparing its value to all of its surrounding neighbours in the same image and in the above and lower scales.

### 2. Keypoint Localization

Refinement is applied to all the interest points and removed if found to be unstable. Unstable points to be removed are those noisy or edge points.

### 3. Orientation Allocation

Location of points can be determined by the identifying the location and the scale. The histogram distribution of the local gradients is determined and the peak value in the histogram is considered the dominant orientation

### 4. Keypoint descriptor

The local image gradients are calculated at particular scale in a box around the key point and transformed into a form that permits for levels of the intensity changing levels and distortion in shapes.

That is to say, the first three steps of the SIFT algorithm assure the location, scale, and rotation variations remain unchanged. The last step assures the invariance for the left parameters such as variation in intensity. The Euclidean distance is measured for every key point in target and source images, and the key point in the source image that achieves the minimum distance is chosen as a matching point.

## 3 Simulation and Results

Four groups of experiments were performed to show the advantages of the DOST over the other similar frequency analysis tools (DCT, DWT). The setup and the results are shown in the next 4 sections. For every experiment new data set is prepared, and training for ANN is performed and results are measured, finally, a comparison is presented. The setup of the experiment is performed on an MRI image which is subjected to geometrical affine transformation. For example, the source image is presented in Fig. 5a and the target image is presented in Fig. 5b. The source image size for our experiments is of size 256\*256 and of 256 grey levels.

For every experiment, every dataset includes DOST coefficients, and SIFT features resulting from different setups. The DOST coefficients are part of the frequency-time domain including only the significant coefficients (100 coefficients in our experiments), While the SIFT features will be limited to part of the matched key points (100 in our experiments).

The used ANN was shown in Fig. 3. The input for this ANN is composed of features from both of spatial and frequency domains. The output is the vector of the geometrical parameters that used for transforming the

image. The used ANN for all the experiments is composed of one hidden layer with 10 neurons for this hidden layer. The input for this hidden layer is composed of 200 features and the output is 5 neurons representing the transformation parameters. Results will be given based on the Root Mean Square Error (RMSE). A detailed result of the performance of every transformation parameter is given in experiment 4. The details include Maximum Absolute Error (MAE) for every individual parameter.

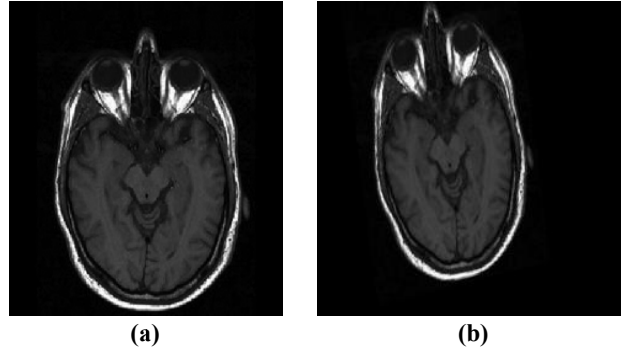


Fig. 5. MRI image before and after deformation

### 3.1 Experiment 1

In this Experiment, transformation parameters are fixed as shown in Table 1 except the rotation angle  $\theta$  which is subject to changes.

Table 1. Input parameters limits for Experiment 1 (Scaling factors and Translation factors)

	Min.	Max.
(Scale factor in x direction) $s_x$	0.9	1.1
(Scale factor in y direction) $s_y$	0.9	1.1
(Translation in x direction) $\Delta_x$	-3	3
(Translation in y direction) $\Delta_y$	-3	3

The used values for the rotation angle ( $\theta$ ) and the resultant RMSE for each is shown in Table 2.

Table 2. Resultant RMSE for (DCT, DOST, and DWT) versus rotation angles

		Experiment 1	Experiment 2	Experiment 3
Rotation angle ( $\theta$ )	Min.	-5	-10	-15
	Max.	5	10	15
RMSE	DCT	0.016	0.047	0.113
	DOST	0.011	0.034	0.086
	DWT	0.101	0.173	0.209

### 3.2 Experiment 2

In this Experiment, transformation parameters are fixed as shown in Table 3 except the translation parameters  $\Delta_x$ , and  $\Delta_y$  which are subject to changes.

The used values for the translation parameters and the resultant RMSE for each is shown in Table 4.



**Table 3. Input parameters limits for Experiment 2 (Rotation angle and scaling factors)**

	<b>Min.</b>	<b>Max</b>
Rotation angle( $\theta$ )	-5	5
(Scale factor in x direction) $s_x$	0.9	1.1
(Scale factor in y direction) $s_y$	0.9	1.1

**Table 4. Resultant RMSE for (DCT, DOST, and DWT) versus Translation parameters**

		<b>Experiment 1</b>	<b>Experiment 2</b>	<b>Experiment 3</b>
Translation in x, y directions $\Delta_x, \Delta_y$	Min.	-3	-6	-9
	Max.	3	6	9
RMSE	DCT	0.016	0.047	0.059
	DOST	0.011	0.028	0.041
	DWT	0.101	0.136	0.215

### 3.3 Experiment 3

In this Experiment, transformation parameters are fixed as shown in Table 3 except the scaling parameters  $s_x$ , and  $s_y$  which are subject to changes.

**Table 5. Input parameters limits for Experiment 3 (Rotation angle and Translation factors)**

	<b>Min.</b>	<b>Max</b>
Rotation angle( $\theta$ )	-5	5
Translation factor in x direction) $\Delta_x$	-3	3
Translation factor in y direction) $\Delta_y$	-3	3

The used values for the translation parameters and the resultant RMSE for each is shown in Table 6.

**Table 6. Resultant RMSE for (DCT, DOST, and DWT) versus scaling factors**

		<b>Experiment 1</b>	<b>Experiment 2</b>	<b>Experiment 3</b>
Scaling factors in x,y directions $s_x, s_y$	Min.	0.85	0.875	0.9
	Max.	1.15	1.125	1.1
RMSE	DCT	0.037	0.037	0.016
	DOST	0.033	0.012	0.011
	DWT	0.146	0.146	0.101

### 3.4 Experiment 4

For testing the estimation of the individual parameters, a specific testing setup is shown in Table 7.

**Table 7. Input parameters limits for Experiment 4**

	<b>Min.</b>	<b>Max</b>
Rotation angle( $\theta$ )	-5°	5°
(Scale factor in x direction) $s_x$	0.9	1.1
(Scale factor in y direction) $s_y$	0.9	1.1
(Translation in x direction) $\Delta_x$	-5	5
(Translation in y direction) $\Delta_y$	-5	5

The resultant RMSE in addition to the MAE for every parameter are shown in Table 8.

**Table 8. Training results (RMSE, and MAE)**

	MAE					RMSE
	$\theta$	$s_x$	$s_y$	$\Delta_x$	$\Delta_y$	
DCT	0.116	0.169	0.203	0.559	0.381	0.055
DOST	0.237	0.074	0.062	0.293	0.577	0.036
DWT	1.037	0.136	0.186	1.178	1.495	0.141

It is obvious that the DOST globally yields a better performance than the DCT and the DWT according to the RMSE. The performance improvement can reach up to 34% better than the DCT and the DWT. Regarding the individual parameters, the scaling parameters  $s_x$  and  $s_x$  show better performance when using the DOST, however, the DCT has a better performance considering the rotation angle  $\theta$ . Both of DCT and DOST perform comparably regarding the translation factors  $\Delta_x, \Delta_y$ . DWT showed the lowest performance among all other domains.

To evaluate the robustness of the proposed algorithm, 300 patterns were selected randomly for testing purposes. A Gaussian noise with different standard deviation (SD) levels ranging from 1 through 10 was added to the image, and the three domains, DCT, DOST and DWT performance indexes were re-evaluated. The results are shown in Fig. 6.

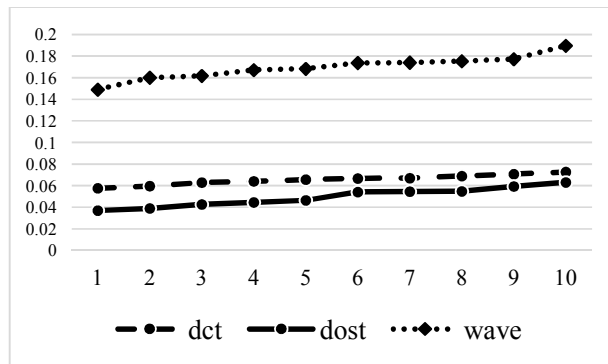


**Fig. 6. RMSE versus SD of added noise**

Fig. 6 shows that the DOST is still superior and more robust on other DCT, and DWT. Table 9 shows the MAE values for the DOST, DCT, and DWT at specifically added noise at SD=10. The table shows that the behaviour of the individual parameters estimation is the same as before.

**Table 9. MAE for affine parameters at SD=10**

	MAE				
	$\theta$	$s_x$	$s_y$	$\Delta_x$	$\Delta_y$
DOST	0.170	0.049	0.050	0.255	0.434
DCT	0.079	0.197	0.173	0.521	0.317
DWT	0.654	0.088	0.138	0.897	0.976

## 4 Conclusion and Future Work

In this research, a new approach for MRI images registration with ANN has been investigated. The output for the ANN is estimating the geometric transformation parameters. The input pattern for training the ANN is composed of a hybrid features obtained from both spatial domain elements, SIFT, and from its frequency

domain components, DOST. A feedforward neural network was used for the training and finally, the trained ANN was tested to evaluate its performance through multiple testing experiments. Two types of testing experiments were conducted, the first is to evaluate the transformation parameters estimation and the second type is to evaluate the estimation's robustness in existence of noise. A comparison between DOST as a base for frequency domain features versus DCT and DWT was performed. The results were evaluated by using two performance indexes, RMSE and MAE. The results showed that the proposed approach is valuable where it provides 34% improvement in RMSE index against DCT. The results also showed robustness against the noise and kept performance advantage over DCT and DWT. This work can be extended in the future to automatically select the optimal number of used patterns and the features.

## Competing Interests

Author has declared that no competing interests exist.

## References

- [1] Kahaki SMM, Nordin MJ, Ashtari AH, Zahra SJ. Invariant feature matching for image registration application based on new dissimilarity of spatial features. PLoS ONE. 2016;11(3):e0149710.
- [2] Song G, Han J, Zhao Y, Wang Z, Du H. Review on medical image registration as an optimization problem. Current Medical Imaging Reviews. 2017;13(3):274–283.
- [3] Zitová B, Flusser J. Image registration methods: A survey. Image and Vision Computing. 2003;21(11):977-1000.
- [4] He K, Yuan Z, Mu C. A new affine transformation parameters estimation method. International Conference on Natural Computation. 2011;28-32.
- [5] Gadde P, Yu XH. Image registration with artificial neural networks using spatial and frequency features. International Joint Conference on Neural Networks (IJCNN). 2016;4643-4649.
- [6] Hartley R, Zisserman A. Multiple view geometry in computer vision. 2<sup>nd</sup> ed. Cambridge University Press; 2004.
- [7] Saxena S, Singh RK. A Survey of recent and classical image registration methods. International Journal of Signal Processing, Image Processing and Pattern Recognition. 2014;7(4):167-176.
- [8] Kumar G, Bhatia PK. A Detailed review of feature extraction in image processing systems. Fourth International Conference on Advanced Computing & Communication Technologies. 2014;5-12.
- [9] Lowe DG. Distinctive image features from scale-invariant keypoints. International Journal of Computer Vision. 2004;60(2):91–110.
- [10] Dawn S, Saxena V, Sharma B. Remote sensing image registration techniques: A survey. International Conference on Image and Signal Processing. 2010;103-112.
- [11] Mahesh, Subramanian MV. Automatic feature based image registration using SIFT algorithm. Computing Communication & Networking Technologies (ICCCNT). 2012;1-5.
- [12] Kokila R, Thangavel P. Image registration based on fast Fourier transform using Gabor filter. International Journal of Computer Science and Electronics Engineering. 2014;2(1):31-37.

- [13] Karani RB, Sarode TK. Image Registration using Discrete Cosine Transform and Normalized Cross Correlation. International Conference and workshop on Emerging Trends in Technology. 2012; 28-34.
- [14] Shakir H, Ahsan ST, Faisal N. Multimodal medical image registration using discrete wavelet transform and Gaussian pyramids. IEEE International Conference on Imaging Systems and Techniques. 2015;1-6.
- [15] Mekky NE, Abou-Chadi FEZ, Kishk S. Wavelet-based image registration techniques: A study of performance. International Journal of Computer Science and Network Security. 2011;11(2):188-196.
- [16] Qu X, Huo H, Lian S, Zhao F. A novel frequency domain iterative image registration algorithm based on local region extraction. Mathematical Problems in Engineering. 2015;1-8.
- [17] Hossein-Nejad Z, Nasri M. Image registration based on SIFT features and adaptive RANSAC transform. 2016;1087-1091.
- [18] El Rube IA, Sharks MA, Salem AR. Image registration based on multi-scale SIFT for remote sensing images. Conference on Signal Processing and Communication Systems;2009:1-5.
- [19] Ye F, Su Y, Xiao H. Remote Sensing image registration using convolutional neural network features. IEEE Geoscience and Remote Sensing Letters. 2018;15(2):232-236.
- [20] Stockwell RG. A basis for efficient representation of the S-transform. Digital Signal Processing. 2007;17(1):371-393.
- [21] Wang Y, Orchard J. Fast discrete orthonormal Stockwell transform. SIAM Journal on Scientific Computing. 2009;31(5):4000–4012.
- [22] Drabycz S, Stockwell RG, Mitchell JR. Image texture characterization using the discrete orthonormal S-transform. Journal of Digital Imaging: The Official Journal of the Society for Computer Applications in Radiology. 2009;22(6):696-708.

---

© 2018 Shamardan; This is an Open Access article distributed under the terms of the Creative Commons Attribution License (<http://creativecommons.org/licenses/by/4.0>), which permits unrestricted use, distribution, and reproduction in any medium, provided the original work is properly cited.

*Peer-review history:*

*The peer review history for this paper can be accessed here (Please copy paste the total link in your browser address bar)*

<http://www.sciencedomain.org/review-history/23885>